High Performance Liquid Crystals for Vehicular Displays

Fenglin Peng*, Yuge Huang*, Fangwang Gou*, Minggang Hu*,

Jian Li**, Zhongwei An**, and Shin-Tson Wu*

*College of Optics and Photonics, University of Central Florida, Orlando, Florida 32816, USA

**Xi'an Modern Chemistry Research Institute, Xi'an 710065, China

Abstract

We report two new liquid crystal mixtures with high clearing point, small visco-elastic coefficient and low activation energy. With overdriving and undershooting approach, the response time is less than 10ms for FFS LCDs at T=0°C and TN at –20°C. Therefore, these mixtures greatly improve the performances of vehicle displays at extreme environments.

Keywords

Liquid crystal material; fast response time; extreme environment durability; vehicle display.

1. Introduction

Several display devices have been widely used in a vehicle, such as instrument cluster display, center information display, and entertainment display [1]. Twisted nematic (TN) [2] and fringing field switching (FFS) [3-5] are two main liquid crystal (LC) modes employed in the vehicle displays. For example, instrument cluster display employs TN LCD since it requires fast response time and high brightness. Besides, the instrument cluster display only exhibits information to the driver, thus viewing angle is not a serious concern. For the center information display (e.g. GPS) and entertainment display for passengers, information sharing and touch panel are preferred. Therefore, FFS LCD is commonly used because it shows advantages in wide view, weak color shift and pressure resistance for touch panels. However, there are two major challenges for vehicle displays in the extreme environment: 1) it requires an LC with high clearing point ($T_c \sim$ 100°C). For other LCD applications (e.g. TV, smartphones and wearable displays), a somewhat lower clearing point (~80°C) is still acceptable [6]. While for displays inside a car, the temperature could easily exceed 80°C during summer time. 2) The displays should remain operational at cold temperature, at least the LC should not freeze at –40°C, while keeping a reasonably fast response time below 0°C [7]. Because during winter time, the displays (e.g. the instrument cluster display and GPS) should remain functional before the car is warmed up. To boost clearing point, three-ring LC compounds are commonly used, which dramatically increases the visco-elastic coefficient and activation energy, resulting in a relative slow response time at low temperature. For electric vehicles, low operation voltage is also very important considering the power consumption.

In this paper, we reported two high performance LC mixtures with an extraordinary wide nematic range (–40°C to ~100°C), small visco-elastic coefficient, and low activation energy for automobile displays. Physical properties at different temperatures and wavelengths are characterized. By applying the LC mixtures to FFS and TN LCDs, the response time is less than 20ms for FFS at 0°C and TN at –20°C, respectively. With overdrive and undershoot voltages [8], the average gray-to-gray (GTG) response time is further reduced by ~2X (<10ms) at these low temperatures. Fast motion picture response time helps to enhance image clarity by reducing image blurs.

2. Physical properties characterization

In experiment, we collaborated with DIC (Japan) and Xi'an (China) and developed two LC mixtures (designated as DIC-57F-16 and MCRI) with high T_c, modest dielectric anisotropy ($\Delta\varepsilon$) yet small visco-elastic coefficient (γ_1/K_{11}) and low activation energy [9]. To obtain wide nematic range, we mixed some fluorinated terphenyl compounds with structure shown in [6] to the mixtures. Besides, we added ~50wt% diluters (also reported in [6]) to lower the viscosity and activation energy. The phase transition temperatures were measured by Differential Scanning Calorimetry (DSC). Remarkably, the melting points (T_m) are below –40°C and clearing point T_c ~100°C for both mixtures, which show high durability in extreme environments.
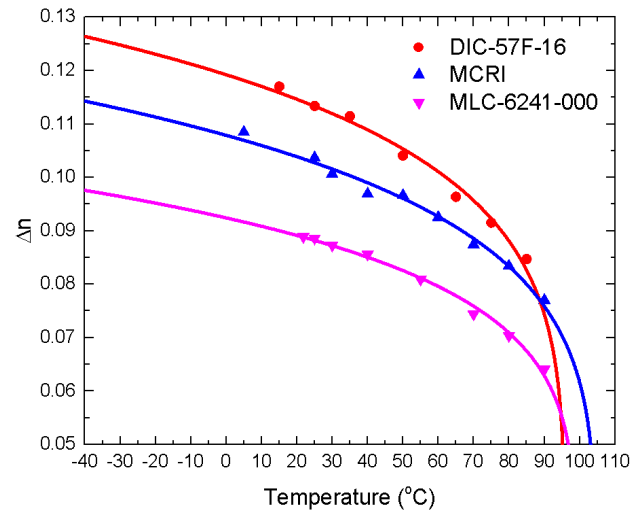

Figure 1. Temperature dependent birefringence of LCs

To characterize the physical properties at different temperatures, we filled each LC into a homogeneous cell with cell gap ($d\sim5\mu m$). A commercial LC (MLC-6241-000) with similar T_c (~98.9°C) was included as a benchmark for comparison. [Caution: This is not the best mixture Merck developed for practical applications, but it is what we have in our laboratory]. The cells were mounted in a Linkam LTS 350 Large Area Heating/Freezing Stage controlled by TMS94 Temperature Programmer and then sandwiched between two crossed polarizers. A 1 kHz square-wave AC voltage was applied to LC cells. The probing light sources are a tunable Argon-ion laser (λ=457nm, 488nm, and 514nm) and a He-Ne laser (λ = 632.8 nm). The birefringence can be obtained from the phase retardation δ=2πdΔn/λ. We also measured their Δn at T=10~90°C as Figure 1 shows. The dots are experimental data and solid curves are theoretical fittings with [10]

$$\Delta n = \Delta n_o S = \Delta n_o (1 - T / T_c)^\beta, \qquad (1)$$

where Δn_o is the extrapolated birefringence at $T=0K$ and the exponent β is a material constant. The Δn of both mixtures is ~0.1, which help minimize the color dispersion for TN and FFS LCDs.

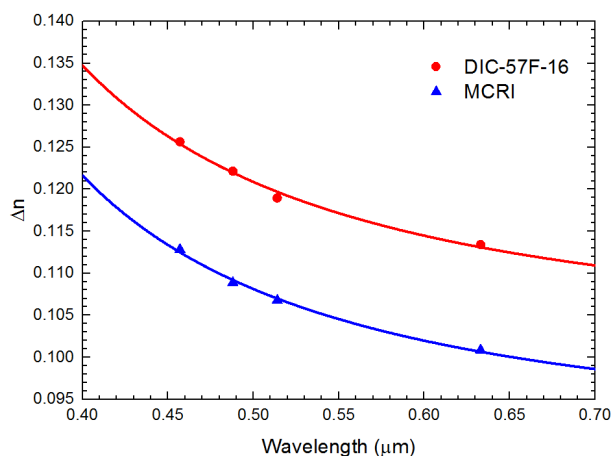**Figure 2.** Birefringence dispersion of two LCs at $T = 25°C$

To investigate the electro-optic performance with different colors, we also fitted the measured Δn (dots in Figure 2) at each wavelength with the single-band dispersion equation [11]:

$$\Delta n = G \frac{\lambda^2 \lambda^{*2}}{\lambda^2 - \lambda^{*2}}. \tag{2}$$

Here, G is a proportionality constant and λ^* is the mean resonance wavelength. Therefore, we found that $\Delta n = 0.12$ and 0.11 at $\lambda=550nm$ for DIC-57F-16 and MCRI respectively, which will be used in the device simulation part later.
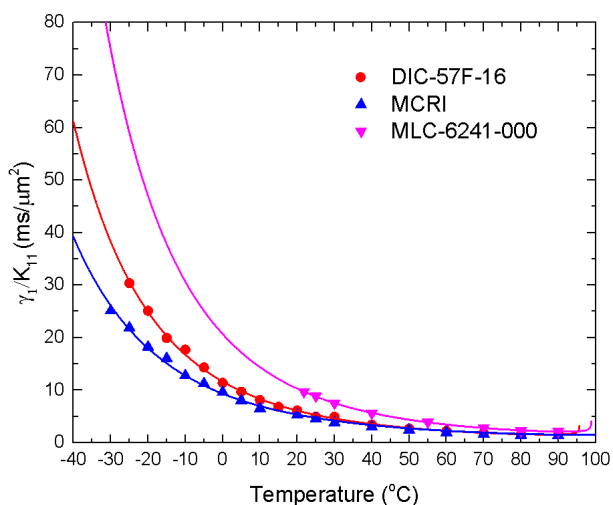

Figure 3. Temperature dependent visco-elastic coefficients of the 3 LC mixtures studied.

Figure 3 depicts the temperature dependent visco-elastic coefficients (γ_1/K_{11}) for three LC mixtures. Each γ_1/K_{11} is obtained by measuring the transient free relaxation time for a controlled phase change. As the temperature decreases, the visco-elastic coefficient increases exponentially. The solid line in Figure 3 is the fitting curve with following equation:

$$\frac{\gamma_1}{K_{11}} = A \frac{\exp(E_a / k_B T)}{(1 - T/T_c)^\beta}, \tag{3}$$

where A is a proportionality constant and E_a is the activation energy. All fitting parameters are listed in **Table 1**. MCRI mixture shows the smallest visco-elastic coefficient and activation energy [12]. As a result, the γ_1/K_{11} of MCRI is ~1.5X smaller than that of MLC-6241-000 at 30°C and ~3X at -30°C.

Table 1. Physical properties and fitting parameters of three LC mixtures studied.

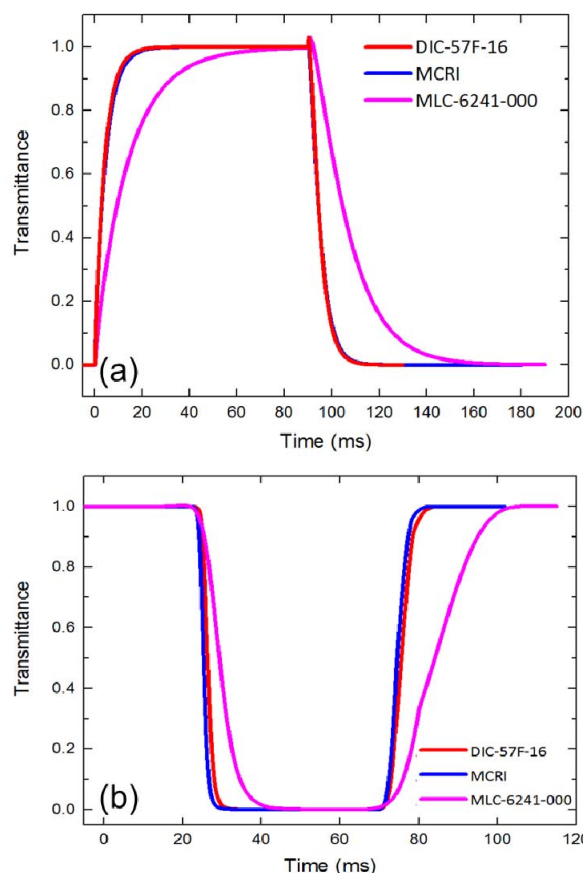|	T_c (°C)	$\Delta\varepsilon$	Δn_0	β	G (μm^{-2})	λ^* (μm)	A ($ms/\mu m^2$)	E_a (meV)
DIC-57F-16	97	4.4	0.15	0.17	2.64	0.20	4.23×10^{-4}	235.7
MCRI	104	4.0	0.14	0.18	2.19	0.20	1.24×10^{-3}	204.9
MLC-6241-000	99	5.5	0.11	0.16	-	-	3.54×10^{-4}	253.7

Figure 4. (a) Time dependent transmittance (TT) curves for FFS mode at $\lambda=550nm$; $d\Delta n=340nm$. (b) TT curves for TN mode at $\lambda=550nm$; $d\Delta n=480nm$ at T=25 °C.

3. Device simulation results

Here, we simulate the electro-optic properties of FFS and TN cells employing our LC materials with a commercial LCD simulator DIMOS.2D and the extended 2x2 Jones matrix method. According to the dispersion curve, $\Delta n=0.12$ and 0.11 for DIC-57F-16 and MCRI at $\lambda=550nm$. For MLC-6241-000, the estimated Δn ~0.09 at $\lambda=550nm$. For FFS mode, we set $d\Delta n$~340nm for each mixture in order to achieve fast response time and low operation voltage. The same cell parameters are used in the simulation for fair comparison: electrode width $w=2\mu m$, electrode gap $l=3\mu m$, pretilt angle ~2° and rubbing

angle ~10°. For TN mode, $d\Delta n$=480nm to satisfy first Gooch-Tarry minimum and to achieve high transmittance. The cells are sandwiched between two crossed polarizers and front rubbing direction is parallel to the axis of polarizer. In both modes, MLC-6241-000 shows the lowest operation voltage due to its larger Δ . The on-state voltages of DIC-57F-16 and MCRI are 6.0V and 6.5V in FFS mode, which are acceptable for vehicle displays. For TN, a good dark state is obtained when V~5V$_{rms}$ for both new LCs. Figures 4(a) and 4(b) depict the response time of FFS and TN at T=25°C. The time dependent transmittance curves of two newly developed LCs are almost the same because of a similar birefringence and visco-elastic coefficient. The response time of our LCs are much faster than that of MLC-6241-000 in both modes. Moreover, the faster response contributes a higher overall transmittance and less image crosstalk. For FFS mode, the response time [rise, decay] of DIC-57F-16 is [9.7ms, 9.3ms], while the response time of MLC-6241-000 is [31.3ms, 31.2ms]. TN shows faster response time than FFS because it utilizes K_{11} while FFS mainly uses K_{22}. Thus, the response time of our LCs is [2.5ms, 5.0ms] for TN, which is ~3.6X faster than that of MLC-6241-000 ([9.0ms, 19.0ms]).

Based on Figure 3, the response time at low temperature can be calculated. Our new LCs show a favorably small activation energy, leading to a much slower rising rate on visco-elastic coefficient as the temperature decreases. At 0°C, the extrapolated decay time of MCRI in FFS cell is still within 20ms, which is ~4X faster than that of MLC-6241-000. Besides, the rise time (i.e. free relaxation) of TN with MCRI is less than 20ms at T= −20°C (for MLC-6241-000, it is longer than 100ms). By using the overdrive and undershoot approach, the average GTG response time is reduced by ~2X. Therefore, by employing our new LCs, the response time is within ~10ms for FFS at T=0°C and TN at T= −20°C. This is particularly important for vehicular displays at cold weather.

4. Conclusion

We reported two new LC mixtures with high T_c, small visco-elastic coefficient, and low activation energy. By employing these LC mixtures, the response time is less than 20ms for FFS at T=0°C and TN at −20°C. With overdrive voltage, the average GTG response could be reduced to below 10 ms at low temperature. It maintained advantages of low operation voltage and high brightness. Thus, these LCs greatly improve the performance of vehicle displays in extreme environments.

6. References

[1] N. Takasaki, T. Harada, A. Sakaigawa, K. Sako, M. Mifune, Y. Shiraishi. "Development of RGBw LCD with edge lit 2D local dimming system for automotive applications," SID Symposium Digest of Technical Papers **46**(1), 616-619 (2015).

[2] M. Schadt, W. Helfrich. "Voltage-dependent optical activity of a twisted nematic liquid crystal," Applied Physics Letters **18**(4), 127-128 (1971).

[3] S. Lee, S. Lee, H. Kim. "Electro-optic characteristics and switching principle of a nematic liquid crystal cell controlled by fringe-field switching," Applied Physics Letters **73**(20), 2881-2883 (1998).

[4] Y. Chen, Z. Luo, F. Peng, S.-T. Wu. "Fringe-field switching with a negative dielectric anisotropy liquid crystal," Journal of Display Technology **9**(2), 74-77 (2013).

[5] M. Engel, G. Bernatz, A. Götz, H. Hirschmann, S. K. Lee. "UB-FFS: New materials for advanced mobile applications," SID Symposium Digest of Technical Papers **46**(1), 645-647 (2015).

[6] Z. Luo, F. Peng, H. Chen, M. Hu, J. Li, Z. An, S.-T. Wu. "Fast-response liquid crystals for high image quality wearable displays," Optical Materials Express **5**(3), 603-610 (2015).

[7] F. Peng, Y. Huang, F. Gou, M. Hu, J. Li, Z. An, S.-T. Wu. "High performance liquid crystals for vehicle displays," Optical Materials Express **6**(3), 717-726 (2016).

[8] S. T. Wu. "Nematic liquid crystal modulator with response time less than 100 μs at room temperature," Applied Physics Letters **57**(10), 986-988 (1990).

[9] H. Takatsu. "Advanced liquid crystal materials for active matrix displays," Conference Proceedings of Advanced Display Materials and Devices, p.43 (2014).

[10] I. Haller. "Thermodynamic and static properties of liquid crystals," Progress in solid state chemistry **10**, 103-118 (1975).

[11] S.-T. Wu. "Birefringence dispersions of liquid crystals," Physical Review A **33**(2), 1270-1274 (1986).

[12] H. Chen, M. Hu, F. Peng, J. Li, Z. An, S.-T. Wu. "Ultra-low viscosity liquid crystal materials," Optical Materials Express **5**(3), 655-660 (2015).